PHYSICAL REVIEW A **106**, 033323 (2022)

Spin-flip-induced superfluidity in a ring of spinful hard-core bosons

K. K. Kesharpu [*] and E. A. Kochetov
Bogoliubov Laboratory of Theoretical Physics, Joint Institute for Nuclear Research, Dubna 141980, Russia

(Received 20 May 2022; revised 18 August 2022; accepted 13 September 2022; published 29 September 2022)

The $t-J$ Hamiltonian of the spinful hard-core bosonic ring in the Nagaoka limit is solved. The energy spectrum becomes quantized due to presence of spin, where each energy level corresponds to a cyclic permutation state of the spin chains. The ground state is true ferromagnetic when the ring contains $N = 2$ and 3 spinful hard-core bosons; for all other N it is a mixture of the ferromagnetic and nonferromagnetic states. This behavior is different from the fermionic ring, where ground state is true ferromagnetic only for $N = 3$. It is shown that the intrinsic spin-generated gauge fields are analogous to the synthetic gauge fields generated by rotation of either the condensate or the confining potential. It is argued that the low-lying excited levels of the spin-flipped states intrinsically support the superfluidity. Possible ways to experimentally verify these results are also discussed.

DOI: 10.1103/PhysRevA.106.033323

I. INTRODUCTION

Rapid progress in the experimental techniques of trapping and manipulating cold atoms has opened numerous possibilities for their use in quantum simulation and quantum computing [1–4]. Spinor bosons—atoms with integer spins—in optical lattice are one of the modern work horses used to probe the physics of the strongly correlated systems [5–7]. They have several advantages over their condensed matter counterparts, e.g., precise knowledge of the underlying microscopic model, the possibility to control the parameters of the lattice Hamiltonian, and the absence of impurity in physical realizations. In this work we theoretically investigate the physics of one of the simplest systems, yet rich in physics, that can be constructed using spinor bosons: the one-dimensional (1D) ring lattice loaded with spinful hard-core bosons (HCBs) [8].

The spinless bosonic ring is a well-studied problem both theoretically and experimentally [6,7,9–11]. In Ref. [11] the Yrast states for fermionic and bosonic ring were given. In Ref. [10] several exactly solvable models for one-dimensional bosonic systems were reviewed. In Ref. [12] a model for neutral *spinless* HCBs on a ring was solved. Reference [13] considered *spinful* HCBs on a $N \times N$ plaquette. On this plaquette they solved the usual *t-J* Hamiltonian by dividing the spinful HCBs into two different species of spinless HCBs. Reference [14] also considered spinful HCBs on a finite 2D plaquette. They investigated the effect of fermionic and bosonic statistics on the emergence of the ferromagnetic phase. In Ref. [15] the phase diagram of a 1D chain, when even and odd numbers of spinful bosons are present at a single site, was investigated. In Refs. [16,17] the ground state properties of the spinful fermions and bosons in thermodynamic limits were studied. Most of the work done till now has been related either to the bosons on one- and two-dimensional periodic lattices, and their behavior in the thermodynamic limit ($N \gg 1$), or to spinless HCBs on a ring. Apart from some comments about the energy levels of the spinful bosonic ring in Ref. [11], a comprehensive study of the properties of the spinful hard-core bosons on a ring away from the thermodynamic limit is still missing.

One of the interesting effects observed in the ring of bosons is the persistent current, which is related to the superfluidity [18–20]. In Ref. [21] the phase diagram of superfluid and insulating phases was studied for spinless hard-core bosons. Reference [22] investigated the ground-state and superfluidic properties of the spinless hard-core bosons in one-dimensional potential. Recently, Ref. [23] estimated the values of persistent current for two hard-core bosons in a ring lattice. From the experimental side the persistent current was observed in spinor (not hard-core) condensates [24] and fermion rings [25,26]. It is well known that the ground state can never support the persistent current [27–29]. Hence, one accesses the excited superfluidic states by applying a velocity field, either by rotating the confined particles in the ring lattice or by rotating the ring lattice itself [18–20,27,28]. The rotation of the lattice is analogous to the generation of synthetic gauge fields, which in turn is related to the twisted boundary condition [18,28]. We show that, for the case of hard-core spinful bosons, the twisted boundary condition is generated intrinsically without application of any external velocity field.

The main focus of our work is the investigation of the ground-state properties and the necessary condition for occurrence of superfluidity in these systems. This article is structured as follows. In Sec. II we solve the Hamiltonian of the spinful HCBs on a ring in the Nagaoka limit. In this limit the spin and charge degrees of freedom can be treated separately; hence, the Hamiltonian is easily solvable. In Sec. III we investigate the dependence of the ground-state energies on the total spin and the structure of the total spin chains. We discuss the necessary conditions for the emergence of superfluidity in these systems. Here, we also suggest the experimental setups to corroborate our theoretical predictions. Finally, In Sec. IV we summarize the results.

[*]kesharpu@theor.jinr.ru

II. THE MODEL

We take a ring of L sites and N spinful HCBs with spin projections $\sigma = \{\uparrow, \downarrow\}$ [30]. Because of the hard-core nature of the bosons, in the ring every site contains *at most a single boson* ($N \leqslant L$). The t-J Hamiltonian in the Nagaoka limit with periodic boundary conditions [31,32] can be written as (see Supplemental Material [33])

$$H = -t \sum_{i=1,\sigma}^{L-1} \tilde{b}_{i\sigma}^{\dagger} \tilde{b}_{i+1\sigma} - t \sum_{\sigma} \tilde{b}_{L\sigma}^{\dagger} \tilde{b}_{1\sigma} + \text{H.c.} \tag{1}$$

Here, t is the boson hopping factor from the ith site to the neighboring $i+1$th site. $\tilde{b}_{i\sigma}^{\dagger}$ and $\tilde{b}_{i\sigma}$ are the HCB creation and annihilation operators with spin projections $\sigma = \{\uparrow, \downarrow\}$. The operators $\tilde{b}_{i\sigma}$ and $\tilde{b}_{i\sigma}^{\dagger}$ imply the single occupancy constraint: $\sum_{\sigma} b_{i\sigma}^{\dagger} b_{i\sigma} \leqslant 1$.

Due to the 1D nature of the ring, and the absence of the spin interaction, the initial spin configuration of the spin chain is fixed during electron hopping. Hence, we can separate the spin and charge degrees of freedom in the Hamiltonian:

$$H = -t \sum_{i=1}^{L-1} b_i^{\dagger} b_{i+1} - t b_L^{\dagger} b_1 \hat{P} + \text{H.c.} \tag{2}$$

Here, $b_i^{\dagger}(b_i)$ is a spinless hard-core bosonic creation (annihilation) operator. The spin content of the problem is encoded in the spin permutation operator $\hat{P}$. It displaces the spin to the next nonempty site:

$$\hat{P} \left| s_1^z, s_2^z, \dots, s_N^z \right\rangle = \left| s_N^z, s_1^z, \dots, s_{N-1}^z \right\rangle.$$

The boson hopping part of Eq. (2) is analogous to the XY spin-chain Hamiltonian [10,12,34,35]. Hence, one can use the Jordan-Wigner transformation to represent the Hamiltonian in Eq. (2) in terms of spinless fermionic operators (see Supplemental Material [33]):

$$H = -t \sum_{i=1}^{L-1} \hat{f}_i^{\dagger} \hat{f}_{i+1} + t e^{\imath \pi N} \hat{f}_L^{\dagger} \hat{f}_1 \hat{P} + \text{H.c.} \tag{3}$$

Here, $\hat{f}_i^{\dagger}$ $(\hat{f}_i)$ is the spinless fermionic creation (annihilation) operator. Defining the function

$$h(N) = \begin{cases} 0, & \text{odd } N, \\ 1, & \text{even } N, \end{cases} \tag{4}$$

we can write Eq. (3) as

$$H = -t \sum_{i=1}^{L-1} \hat{f}_i^{\dagger} \hat{f}_{i+1} - t e^{\imath \pi h(N)} \hat{f}_L^{\dagger} \hat{f}_1 \hat{P} + \text{H.c.} \tag{5}$$

The spin permutation and spinless fermionic operators are separately diagonalized, because they are independent of each other. The eigenvalues (λ_ν) and eigenfunction (ψ_ν) of $\hat{P}$ are [36]

$$\lambda_\nu = e^{\imath 2\pi p_\nu / N_\nu}, \tag{6a}$$

$$|\psi_\nu\rangle = \frac{1}{\sqrt{N_\nu}} \sum_{q=0}^{N_\nu - 1} e^{\imath 2\pi p_\nu \frac{q}{N_\nu}} \hat{P}^q \, |\tilde{\psi}_\nu\rangle \,. \tag{6b}$$

Here, ν enumerates all possible disconnected spin blocks. A spin block contains only connected spin chains. When two spin chains can be transformed into each other by application of the $\hat{P}$ operator they are connected; otherwise they are disconnected. N_ν represents the total number of connected spin chains in the νth spin block. p_ν enumerates the connected spin chains in the νth spin block; it takes the values $p_\nu = 0, 1, \dots, N_\nu - 1$. $\tilde{\psi}_\nu$ is the wave function of one of the spin chains of the νth spin block.

For example, we have a chain of four sites and three particles. We take the spin chain $|\uparrow \bullet \uparrow \downarrow\rangle$ out of 2^3 possible spin chains. It is connected to the $|\uparrow \bullet \downarrow \uparrow\rangle$ spin chain, as $\hat{P}^2 \, |\uparrow \bullet \uparrow \downarrow\rangle = |\uparrow \bullet \downarrow \uparrow\rangle$. In this case both these configurations belong to the same νth spin block. This particular νth block has three possible configurations; hence $N_\nu = 3$, and $p_\nu = 0$, 1, and 2 [37]. The wave function of three p_ν states can be found using Eq. (6b) [see Appendix C]. Consequently, every spin chain in the νth spin block has its own wave function and spin momentum p_ν. The number of disconnected blocks depends on the number of particles present in the ring (N) and the spin of these particles (s^z). Due to these disconnected blocks of spin chains, the total spin Hamiltonian corresponding to the $\hat{P}$ operator is a block Hamiltonian with ν blocks. We find the Hamiltonian corresponding to the νth block by substituting λ_ν from Eq. (6b) into Eq. (5):

$$H_\nu = -t \sum_{i=1}^{L-1} \hat{f}_i^{\dagger} \hat{f}_{i+1} - t e^{i2\pi [\frac{p_\nu}{N_\nu} + \frac{h(N)}{2}]} \hat{f}_L^{\dagger} \hat{f}_1 + \text{H.c.} \tag{7}$$

The total Hamiltonian of the whole system is a direct sum of these spin-block Hamiltonians: $H = \sum_{\nu} \oplus H_\nu$.

Equation (7) is nothing but the tight -binding model with a penetrating magnetic flux $\Phi_\nu \equiv 2\pi[\frac{p_\nu}{N_\nu} + \frac{h(N)}{2}]$ through the ring. Using the gauge $f_i \mapsto e^{\imath \Phi_\nu x_i / L} f_i$, one maps the Hamiltonian in Eq. (7) onto the twisted Hamiltonian:

$$H_\nu = -t \sum_{i}^{L-1} e^{\imath \frac{\Phi_\nu}{L}} \hat{f}_i^{\dagger} \hat{f}_{i+1} - t e^{\imath \frac{\Phi_\nu}{L}} \hat{f}_L^{\dagger} \hat{f}_1 + \text{H.c.} \tag{8}$$

Here, $x_i = 1, 2, \dots, L$, enumerates the L sites. The locally induced phase factor $e^{\imath \Phi_\nu / L}$ is known as the Peierls phase. The explicit expression for the kth mode energy of this tight-binding Hamiltoinian H_ν is (see Supplemental Material [33])

$$E_{\text{PBC}}(k, \nu, p_\nu; N, L) = -2t \cos \frac{2\pi}{L} \left(k + \frac{p_\nu}{N_\nu} + \frac{h(N)}{2} \right). \tag{9}$$

The total energy is found by summing over all N low-lying kth mode energies:

$$E_{\mathrm{PBC},\,g} = -2t\frac{\sin\{[N+1+h(N)]\pi/2L\}}{\sin(\pi/L)} \times \cos\left[\frac{\frac{4\pi}{L}\left(\frac{p_\nu}{N_\nu}+\frac{h(N)}{2}\right)+\frac{[N-1+h(N)]\pi}{L}}{2}\right] - 2t\frac{\sin\{[N+1+h(N)]\pi/2L\}}{\sin(\pi/L)} \times \cos\left[\frac{\frac{4\pi}{L}\left(\frac{p_\nu}{N_\nu}+\frac{h(N)}{2}\right)-\frac{[N-1+h(N)]\pi}{L}}{2}\right] + 2t[1+h(N)]\cos\left[\frac{2\pi}{L}\left(\frac{p_\nu}{N_\nu}+\frac{h(N)}{2}\right)\right]. \quad (10)$$

The Hamiltonian of the antiperiodic boundary condition ($\tilde{b}_{L+1,\sigma} = -\tilde{b}_{1,\sigma}$) is written by introducing the extra phase $e^{i\pi}$ in the second term of Eq. (1). Repeating the aforementioned procedure, the kth mode energy levels and the ground-state energies can be calculated. One can directly find these expressions from Eqs. (9) and (10) by replacing $h(N) \to h(N+1)$. If a magnetic field $\mathbf{B}$ is applied perpendicular to the ring, then an additional flux $\Phi_B = 2\pi\mathbf{B}A$—where A is the area of the ring—penetrates through the ring. To find the total energy one repeats the above calculation by substituting $\Phi_\nu \mapsto \Phi_\nu + \Phi_B$ and adds the total-spin (S_ν)-dependent Zeeman energy, $Z = g\mu_B B S_\nu$ (see Supplemental Material [33]). Here, g is the Lande factor; μ_B is the Bohr magneton; and S_ν is the total spin of the νth block.

III. GROUND-STATE PROPERTIES AND SUPERFLUIDITY

In a ring geometry the energy levels corresponding to the cyclic permutation (p_ν) of the initial spin configurations become available, because particles can jump directly from the Lth site to the 1-st site. One can further group these permutation states into irreducible representations of the cyclic symmetry groups C_n. It should be noted that a single cyclic group can contain more than one spin block (ν). For example, for $N = 4$ the C_4 group contains the $\nu = 2$ and 3 spin blocks as shown in Table I. The more general relation between N, p_ν, and ν can be found using Burnside's Lemma [38].

We show the detailed spin configurations for $N = 4$ and 5 in Tables I and II, respectively. The corresponding energy levels with $L = 8$ are shown in Fig. 1. Here, for $N \geqslant 4$ the ground state is a mixture of the ferromagnetic phase ($S = N/2$) and the nonferromagnetic phases ($S = N/2-2, N/2-3, \dots$). It should be noted that the single spin-flipped phase ($S = N/2-1$) is absent in the ground state due to the unavailability of the $p_\nu = 0$ state (see Appendix A). Interestingly for $N = 2$ and 3, the ground state is pure ferromagnetic, because the spin-flipped phases ($S = N/2-2, N/2-3, \dots$) are not available. This behavior is different from that of the fermionic ring, for which the ground state is pure ferromagnetic only for $N = 3$ [36].

Physically the spinful hard-core bosonic ring can be realized by loading spinor bosons [39,40] in optical tweezers [41–43] or Paul traps [44,45]. The two hyperfine states (F) of the spinor bosons can be considered as two *pseudospin* states. Recently numerous experiments have successfully generated several 2D and 3D crystals with high fidelity [46–51]. Hence, generating 1D rings should not be difficult. One of the interesting facts to observe experimentally is the dependence of the energy levels on underlying spin structures. For example, one can generate a ring of spinor bosons with the initial spin configuration $|\uparrow\uparrow\downarrow\downarrow\rangle$ ($\nu = 3$ in Table I). Then the

TABLE I. The spin configurations for $N = 4$ bosons. Column S represents the total spin of the chain. Column ν represents the enumerated spin blocks. N_ν represents the total number of connected spin chains contained in the νth spin block. p_ν enumerates the connected spin chains in the νth block.

S	ν	N_ν
2	1	$N_1 = 1$
		$p_1 = 0 \equiv \lvert\uparrow\uparrow\uparrow\uparrow\rangle$
1	2	$N_2 = 4$
		$p_2 = 0 \equiv \lvert\uparrow\uparrow\uparrow\downarrow\rangle$
		$p_2 = 1 \equiv \lvert\downarrow\uparrow\uparrow\uparrow\rangle$
		$p_2 = 2 \equiv \lvert\uparrow\downarrow\uparrow\uparrow\rangle$
		$p_2 = 3 \equiv \lvert\uparrow\uparrow\downarrow\uparrow\rangle$
0	3	$N_3 = 4$
		$p_3 = 0 \equiv \lvert\uparrow\uparrow\downarrow\downarrow\rangle$
		$p_3 = 1 \equiv \lvert\downarrow\uparrow\uparrow\downarrow\rangle$
		$p_3 = 2 \equiv \lvert\downarrow\downarrow\uparrow\uparrow\rangle$
		$p_3 = 3 \equiv \lvert\uparrow\downarrow\downarrow\uparrow\rangle$
	4	$N_4 = 2$
		$p_4 = 0 \equiv \lvert\uparrow\downarrow\uparrow\downarrow\rangle$
		$p_4 = 1 \equiv \lvert\downarrow\uparrow\downarrow\uparrow\rangle$

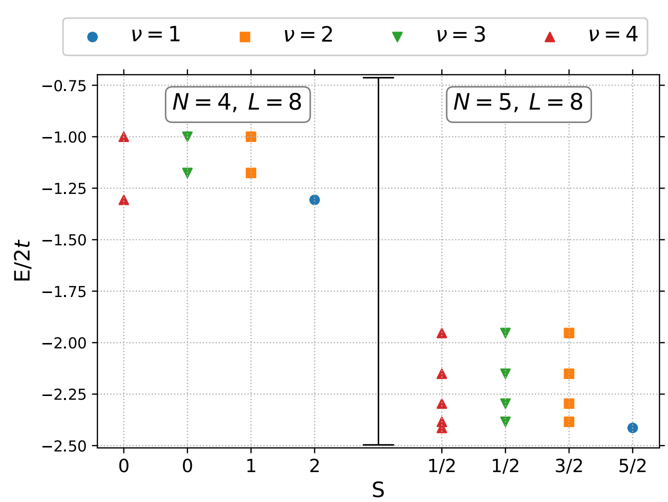

FIG. 1. Energy levels for the periodic boundary condition when $N = 4$ and 5 bosons reside on a ring of $L = 8$ sites. The x axis represents the spin (S), and the y axis represents the energy ($E/2t$). ν represents the spin block. The spin-chain configurations corresponding to different S and ν are shown in Tables I and II. For $\nu = 2$ (squares, orange) and $\nu = 3$ (down triangles, green) the $p_\nu = 0$ state is not available [see Appendix A]. For both $S = 0$ and $S = 1/2$ spin states, there are two corresponding spin blocks: $\nu = 3$ (down triangles, green) and $\nu = 4$ (up triangles, red).

system is excited to the higher energy levels ($p_\nu = 1, 2, 3$) through rotation of the confining potentials [18,19]. To return to the ground state the system should radiate the energy proportional to $E(p_\nu) - E(p_\nu = 0)$, which can be easily measured. In the next step one can prepare the system with the spin arrangement $|\uparrow\downarrow\uparrow\downarrow\rangle$ ($\nu = 4$ in Table I). Analogously the system will be excited to the higher energy levels, and the radiated energy will be measured. In the former case the radiated energy will be higher than that of the latter case, because only a single $p_\nu = 1$ state is available. It will be the direct experimental evidence of the spin-chain-configuration-dependent quantization of the energy in the spinful hard-core bosonic rings.

As an example of the physics displayed by the spinful hard-core bosonic ring, let us show that a slight change of the underlying spin structure of the HCBs on a ring might provide a necessary condition for a superfluidity to emerge. According to the two-fluid picture, the superfluid contains both normal as well as superfluid components. One therefore defines a quantity, the so-called *superfluid fraction* (f_s), to represent the *degree of superfluidity*. There are different ways to calculate it [28,52]. We use the definition where f_s is calculated through the reaction of the system under a change in boundary conditions. Mathematically, the change in boundary conditions is equivalent to imposing a linear phase variation $\Theta x/L$ over length L of the system [28]. Hence, if $\Psi(x)$ is the wave function of the superfluid, then $\Psi(x + L) = e^{i\Theta}\Psi(x)$. It should be stressed that the phase variation should be linear in x to conserve the symmetry of the system and avoid a phase slip. Physically it means that the particles acquire a similar phase Θ/L while tunneling to the neighboring sites. Physically, the twisted phase Θ is imposed by rotating the system with some angular velocity ω [28,53,54]. For a unit radius 1D ring, Θ is related to the superfluid velocity: $v_s = \hbar\Theta/(mL)$ [28,29,54]. Experimentally, the twisted phase can be imposed through atom-light interactions [55], rotating the confining potential [18], or rotating the confined atoms [19]. However, there is another way to impose the twisted boundary condition: through the change in the underlying spin configurations. Indeed the phase factor Φ_ν/L in Eq. (8), which is dependent on the spin configuration through ν, is equivalent to the twisted phase. The persistent current appears when $\Phi_\nu \ll \pi$, because only for this case the high-energy excitation is absent in the system [53]. In this limit the superfluid density is [54]

$$f_s = \frac{L^2}{tN}\frac{E_{\Phi_\nu} - E_0}{\Phi_\nu^2}. \tag{11}$$

Here, E_0 (E_{Φ_ν}) is the energy of the system in the absence (presence) of the phase twist.

Equation (11) is directly applicable when the ring contains *odd and large* numbers of particles. In this case the low-lying excited energy levels ($p_\nu \ll N_\nu$) satisfy the condition $\Phi_\nu^{\text{odd}} := 2\pi p_\nu/N_\nu \ll \pi$. For even N, the twisted phase takes on the form $\Phi_\nu^{\text{even}} := 2\pi p_\nu/N_\nu + \pi$. An extra phase factor of π accounts for a passage from odd N to even N. Therefore, to calculate f_s induced solely by a change in the spin structure at fixed even N, we should replace $\Phi_\nu^{\text{even}} \mapsto \Phi_\nu^{\text{even}} - \pi = \Phi^{\text{odd}} \ll \pi$. In Fig. 2 we plotted the dependence of the superfluid fraction on the number of sites in the ring for $N \geqslant 5$ and $p_\nu/N_\nu = 1/N$. It can be observed that, when $N \approx L$ (commensurate), superfluidity is absent ($f_s \approx 0$). However, the superfluid fraction increases as L increases (incommensurate). The occurrence of the superfluidity for the incommensurate case ($N/L \ll 1$) is a manifestation of the fact that a 1D dilute gas of hard-core bosons is always superfluid [28].

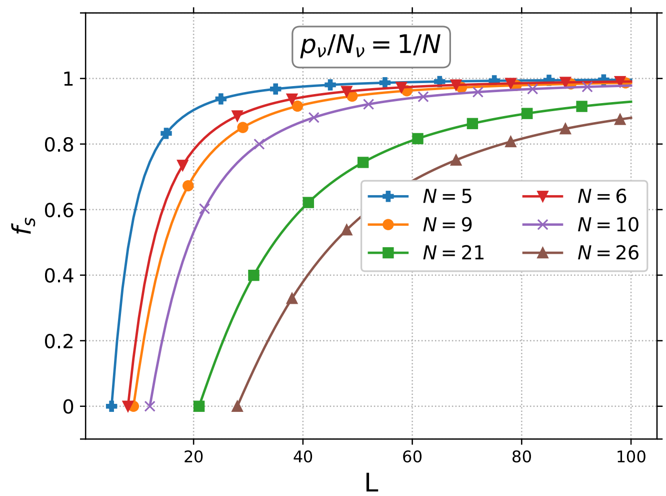

FIG. 2. Dependence of superfluid fraction (f_s) on number of sites (L) while number of particles (N) is fixed. f_s is calculated using Eq. (11) with phase $\theta = 2\pi/N$ for $N = 5$ (blue, plus), $N = 6$ (red, down-triangle), $N = 9$ (orange, circle), $N = 10$ (violet, cross), $N = 21$ (green, square), and $N = 26$ (brown, up-triangle).

It should be mentioned that the condition $\Phi_\nu \ll \pi$, is *necessary but not sufficient* for the appearance of superfluidity, because it does not say anything about the stability of the persistent currents [27]. We propose the following experiment to detect superfluidity generated by a single spin-flip. One can prepare a 1D ring of spinor bosons using optical tweezers, and containing $N \gg 1$. All the particles should be in the same spin state; in other words, the system is in the ferromagnetic phase ($S = N/2$). Then the spin of a single atom is flipped. Due to the absence of the $p_\nu = 0$ state for spin $S = N/2 - 1$, the ground state will then be the first excited state ($p_\nu = 1$). It is equivalent to generating a small twisted phase $\Phi = 2\pi/N$. One can then experimentally find the *matter-wave interference pattern* and *structure factor* to get information about superfluidity [53].

IV. CONCLUSIONS

We have shown that in the spinful hard-core bosonic ring energy spectrum is quantized. Here each excited energy level corresponds to a cyclic permutation state (p_ν) of the spin chain. Interestingly, depending on the underlying spin configuration of the spin chains, the spin blocks with identical total spin (S) can have different sizes (N_ν). For example, although the total spin of the spin-chains $|\uparrow\uparrow\downarrow\downarrow\rangle$ and $|\uparrow\downarrow\uparrow\downarrow\rangle$ are same ($S = 0$), however due to different spin configurations the size of the corresponding spin blocks will be 4 and 2 respectively (see Table I). To corroborate this fact, one can perform experiments measuring the radiated energy from the first excited state ($p_\nu = 1$) to the ground states. For $|\uparrow\uparrow\downarrow\downarrow\rangle$ the radiated energy will always be lower compared to $|\uparrow\downarrow\uparrow\downarrow\rangle$. We have shown that the ground phase of the bosonic ring is true ferromagnetic only for $N = 2$ and 3. This is important, because for the fermionic ring the ground state is true ferromagnetic only for $N = 3$. Usually the superfluid fraction is measured by measuring the energy change due to the imposed twisted phase $\Phi_\nu \ll \pi$. We have shown that apart from already existing methods for generating the twisted phase—rotation of either the condensate or the confining potential, and the light atom interaction—one can use the spin-generated intrinsic phases $2\pi p_\nu/N_\nu$ as a twisted phase. This provides another way to generate the twisted phase in hard-core bosonic rings. We argue that the low-lying energy levels occurring due to cyclic permutation of the spin chains ($p_\nu \ll N$) can support the persistent current without any external excitation, when (i) $N \gg 1$ and (ii) $N/L \ll 1$. In other words, superfluid emerges spontaneously during the transition from the fully polarized state ($S = N/2$) to the spin-flipped states. In this article we have also proposed several experiments to corroborate the above-mentioned results.

ACKNOWLEDGMENTS

This article is partly supported by the RFBR under Grant No. 21-52-12027. K.K.K. would like to thank Pavel D. Grigoriev for useful discussion on the problem.

APPENDIX A: UNAVAILABILITY OF $p_\nu = 0$ STATE FOR $S = (N/2) - 1$

For the case of $p_\nu = 0$ the spin wave function $|\psi\rangle$ in Eq. (6b) is symmetric. It corresponds to the fully polarized case. Hence, if we have x number of $p_\nu = 0$ states, then one of the $p_\nu = 0$ states corresponds to the fully polarized case, and $x - 1$ number of $p_\nu = 0$ states correspond to the spin-flipped case. For example, we take a ring with five spinful HCBs ($N = 5$). The spin configurations for $N = 5$ is shown in Table II. Here we observe that for $S = 5/2$ a single $p_\nu = 0$ state is available, for $S = 3/2$ a single $p_\nu = 0$ state is available, and for $S = 1/2$ two $p_\nu = 0$ states are available. For $S = 3/2$ no $p_\nu = 0$ state is available, because the single $p_\nu = 0$ corresponds to the fully polarized (ferromagnetic) state. However, for $S = 1/2$, because two $p_\nu = 0$ states are available, one $p_\nu = 0$ state corresponds to the fully polarized (ferromagnetic) state, and the other $p_\nu = 0$ state corresponds to the nonferromagnetic phase.

APPENDIX B: SPIN CONFIGURATIONS FOR $N = 4$ AND $N = 5$ SPINFUL HCB ON A RING

In Table I we represent all possible spin configurations of four spinful HCBs. It should be noted that number of sites L does not have any effect on the spin configurations. In Table II we represent all possible spin configurations of five spinful HCBs.

TABLE II. The spin configurations for $N = 5$ bosons. Column S represents the total spin of the chain. Column ν represents the enumerated spin blocks. N_ν represents the total number of connected spin chains contained in the νth spin block. p_ν enumerates the connected spin chains in the νth block.

S	ν	N_ν
$\frac{5}{2}$	1	$N_1 = 1$
		$p_1 = 0 \equiv \|\uparrow\uparrow\uparrow\uparrow\uparrow\rangle$
$\frac{3}{2}$	2	$N_2 = 5$
		$p_2 = 0 \equiv \|\uparrow\uparrow\uparrow\uparrow\downarrow\rangle$
		$p_2 = 1 \equiv \|\downarrow\uparrow\uparrow\uparrow\uparrow\rangle$
		$p_2 = 2 \equiv \|\uparrow\downarrow\uparrow\uparrow\uparrow\rangle$
		$p_2 = 3 \equiv \|\uparrow\uparrow\downarrow\uparrow\uparrow\rangle$
		$p_2 = 4 \equiv \|\uparrow\uparrow\uparrow\downarrow\uparrow\rangle$
$\frac{1}{2}$	3	$N_3 = 5$
		$p_3 = 0 \equiv \|\uparrow\uparrow\uparrow\downarrow\downarrow\rangle$
		$p_3 = 1 \equiv \|\downarrow\uparrow\uparrow\uparrow\downarrow\rangle$
		$p_3 = 2 \equiv \|\downarrow\downarrow\uparrow\uparrow\uparrow\rangle$
		$p_3 = 3 \equiv \|\uparrow\downarrow\downarrow\uparrow\uparrow\rangle$
		$p_3 = 4 \equiv \|\uparrow\uparrow\downarrow\downarrow\uparrow\rangle$
	4	$N_4 = 5$
		$p_4 = 0 \equiv \|\uparrow\uparrow\downarrow\uparrow\downarrow\rangle$
		$p_4 = 1 \equiv \|\downarrow\uparrow\uparrow\downarrow\uparrow\rangle$
		$p_4 = 2 \equiv \|\uparrow\downarrow\uparrow\uparrow\downarrow\rangle$
		$p_4 = 3 \equiv \|\downarrow\uparrow\downarrow\uparrow\uparrow\rangle$
		$p_4 = 4 \equiv \|\uparrow\downarrow\uparrow\downarrow\uparrow\rangle$

APPENDIX C: MATRIX REPRESENTATION OF SPIN WAVE FUNCTION

For a spin-chain configuration $|\uparrow\bullet\uparrow\downarrow\rangle$, using Eq. (6b), the wave functions of the spin chain can be represented in a compact form using the matrix notation $|\psi(p_\nu)\rangle = (1/\sqrt{N_\nu})C\,|\tilde{\psi}_\nu\rangle$. Here $|\psi(p_\nu)\rangle$ is a $N_\nu \times 1$ column matrix. Its components represent the wave function corresponding to the p_νth value. C is the $N_\nu \times N_\nu$ matrix. Its rows and columns are indexed as $p_\nu = 0, 1, \ldots N_\nu$. Hence, the C_{mn}th term is $e^{\imath 2\pi m(n/N_\nu)}$. The wave function $|\tilde{\psi}_\nu\rangle$ is an $N_\nu \times 1$ column matrix of all possible connected spin chains of the νth block. If the νth block represents all the connected spin chains of $|\uparrow\bullet\uparrow\downarrow\rangle$, the total wave function of the νth block is

$$\begin{bmatrix}\psi_\nu(p_\nu=0)\\ \psi_\nu(p_\nu=1)\\ \psi_\nu(p_\nu=2)\end{bmatrix} = \frac{1}{\sqrt{N_\nu}}\begin{bmatrix}1 & 1 & 1\\ 1 & e^{\imath 2\pi/3} & e^{\imath 4\pi/3}\\ 1 & e^{\imath 4\pi/3} & e^{\imath 8\pi/3}\end{bmatrix}\begin{bmatrix}|\uparrow\bullet\uparrow\downarrow\rangle\\ |\downarrow\bullet\uparrow\uparrow\rangle\\ |\uparrow\bullet\downarrow\uparrow\rangle\end{bmatrix}. \tag{C1}$$

Equation (C1) can be generalized to arbitrary N.

[1] I. M. Georgescu, S. Ashhab, and F. Nori, Rev. Mod. Phys. **86**, 153 (2014).

[2] C. D. Bruzewicz, J. Chiaverini, R. McConnell, and J. M. Sage, Appl. Phys. Rev. **6**, 021314 (2019).

[3] F. Schäfer, T. Fukuhara, S. Sugawa, Y. Takasu, and Y. Takahashi, Nat. Rev. Phys. **2**, 411 (2020).
[4] I. Bloch, Nat. Phys. **1**, 23 (2005).
[5] I. Bloch, J. Dalibard, and S. Nascimbène, Nat. Phys. **8**, 267 (2012).
[6] I. Bloch, J. Dalibard, and W. Zwerger, Rev. Mod. Phys. **80**, 885 (2008).
[7] M. Lewenstein, A. Sanpera, V. Ahufinger, B. Damski, A. Sen(De), and U. Sen, Adv. Phys. **56**, 243 (2007).
[8] When two or more bosons cannot occupy the same position due to strong repulsive interparticle potential, they are known as hard-core bosons [56].
[9] O. Morsch and M. Oberthaler, Rev. Mod. Phys. **78**, 179 (2006).
[10] M. A. Cazalilla, R. Citro, T. Giamarchi, E. Orignac, and M. Rigol, Rev. Mod. Phys. **83**, 1405 (2011).
[11] M. Manninen, S. Viefers, and S. Reimann, Phys. E **46**, 119 (2012).
[12] Z. D. Wang and J.-X. Zhu, Phys. Rev. B **52**, 5275 (1995).
[13] M. Boninsegni, Phys. Rev. Lett. **87**, 087201 (2001).
[14] A. Fledderjohann, A. Langari, E. Müller-Hartmann, and K.-H. Mütter, Eur. Phys. J. B **43**, 471 (2005).
[15] S. Bergkvist, I. P. McCulloch, and A. Rosengren, Phys. Rev. A **74**, 053419 (2006).
[16] W. Nie, H. Katsura, and M. Oshikawa, Phys. Rev. B **97**, 125153 (2018).
[17] W. Nie, H. Katsura, and M. Oshikawa, Phys. Rev. Lett. **111**, 100402 (2013).
[18] N. Cooper, Adv. Phys. **57**, 539 (2008).
[19] A. L. Fetter, Rev. Mod. Phys. **81**, 647 (2009).
[20] S. I. Vilchynskyy, A. I. Yakimenko, K. O. Isaieva, and A. V. Chumachenko, Low Temp. Phys. **39**, 724 (2013).
[21] X. Cai, S. Chen, and Y. Wang, Phys. Rev. A **81**, 023626 (2010).
[22] Y. Lin and B. Wu, Phys. Rev. A **75**, 023613 (2007).
[23] J. Polo, P. Naldesi, A. Minguzzi, and L. Amico, Phys. Rev. A **101**, 043418 (2020).
[24] S. Beattie, S. Moulder, R. J. Fletcher, and Z. Hadzibabic, Phys. Rev. Lett. **110**, 025301 (2013).
[25] J. K. Chin, D. E. Miller, Y. Liu, C. Stan, W. Setiawan, C. Sanner, K. Xu, and W. Ketterle, Nature (London) **443**, 961 (2006).
[26] Y. Cai, D. G. Allman, P. Sabharwal, and K. C. Wright, Phys. Rev. Lett. **128**, 150401 (2022).
[27] L. P. Pitaevskiĭ and S. Stringari, *Bose-Einstein Condensation and Superfluidity*, 1st ed., International Series of Monographs on Physics No. 164 (Oxford University, Oxford, 2016).
[28] E. H. Lieb, R. Seiringer, and J. Yngvason, Phys. Rev. B **66**, 134529 (2002).
[29] A. J. Leggett, Rev. Mod. Phys. **71**, S318 (1999).
[30] Although the bosons do not have two spin projections $\pm 1/2$ like fermions, two *hyperfine* states of some atoms can be considered as two spin projections of the bosons. These spins are known as the *pseudospins*, and these atoms are known as the *spinor bosons* [39,40]. Naturally, one can map the *pseudospins* to the spin-up state ($|\uparrow\rangle$) and the spin-down state ($|\downarrow\rangle$).
[31] Y. Nagaoka, Phys. Rev. **147**, 392 (1966).
[32] Y. Nagaoka, Solid State Commun. **3**, 409 (1965).
[33] See Supplemental Material at http://link.aps.org/supplemental/10.1103/PhysRevA.106.033323 for the pedagogical solution of the Hamiltonian, detailed calculation of energy levels, and effect of magnetic field on energy level.
[34] T. Holstein and H. Primakoff, Phys. Rev. **58**, 1098 (1940).
[35] E. Lieb, T. Schultz, and D. Mattis, Ann. Phys. **16**, 407 (1961).
[36] I. Ivantsov, H. B. Xavier, A. Ferraz, and E. Kochetov, Phys. Rev. B **101**, 195107 (2020).
[37] The three configurations ($N_\nu = 3$) corresponding to three p_ν are (i) $p_\nu = 0 \equiv |\uparrow \bullet \uparrow\downarrow\rangle$, (ii) $p_\nu = 1 \equiv |\downarrow \bullet \uparrow\uparrow\rangle$, and (iii) $p_\nu = 2 \equiv |\uparrow \bullet \downarrow\uparrow\rangle$.
[38] H. B. Xavier, E. Kochetov, and A. Ferraz, Phys. Rev. B **101**, 045112 (2020).
[39] D. M. Stamper-Kurn and M. Ueda, Rev. Mod. Phys. **85**, 1191 (2013).
[40] Y. Kawaguchi and M. Ueda, Phys. Rep. **520**, 253 (2012).
[41] D. G. Grier, Nature (London) **424**, 810 (2003).
[42] K. C. Neuman and S. M. Block, Rev. Sci. Instrum. **75**, 2787 (2004).
[43] M. de Goër de Herve, Y. Guo, C. De Rossi, A. Kumar, T. Badr, R. Dubessy, L. Longchambon, and H. Perrin, J. Phys. B: At., Mol. Opt. Phys. **54**, 125302 (2021).
[44] C. Schneider, D. Porras, and T. Schaetz, Rep. Prog. Phys. **75**, 024401 (2012).
[45] M. Tomza, K. Jachymski, R. Gerritsma, A. Negretti, T. Calarco, Z. Idziaszek, and P. S. Julienne, Rev. Mod. Phys. **91**, 035001 (2019).
[46] F. Nogrette, H. Labuhn, S. Ravets, D. Barredo, L. Béguin, A. Vernier, T. Lahaye, and A. Browaeys, Phys. Rev. X **4**, 021034 (2014).
[47] D. Barredo, V. Lienhard, S. de Léséleuc, T. Lahaye, and A. Browaeys, Nature (London) **561**, 79 (2018).
[48] D. Barredo, S. de Léséleuc, V. Lienhard, T. Lahaye, and A. Browaeys, Science **354**, 1021 (2016).
[49] M. Endres, H. Bernien, A. Keesling, H. Levine, E. R. Anschuetz, A. Krajenbrink, C. Senko, V. Vuletic, M. Greiner, and M. D. Lukin, Science **354**, 1024 (2016).
[50] H. Kim, W. Lee, H.-g. Lee, H. Jo, Y. Song, and J. Ahn, Nat. Commun. **7**, 13317 (2016).
[51] M. D'Onofrio, Y. Xie, A. J. Rasmusson, E. Wolanski, J. Cui, and P. Richerme, Phys. Rev. Lett. **127**, 020503 (2021).
[52] N. V. Prokof'ev and B. V. Svistunov, Phys. Rev. B **61**, 11282 (2000).
[53] R. Roth and K. Burnett, Phys. Rev. A **68**, 023604 (2003).
[54] R. Roth and K. Burnett, Phys. Rev. A **67**, 031602(R) (2003).
[55] J. Dalibard, F. Gerbier, G. Juzeliūnas, and P. Öhberg, Rev. Mod. Phys. **83**, 1523 (2011).
[56] M. Girardeau, J. Math. Phys. **1**, 516 (1960).